Model Tests of Spinning Turbine Fragments on Casing Models

J.S. Wilbeck

Southwest Research Institute, P.O. Drawer 28510, San Antonio, Texas 78284, U.S.A.

Summary

A series of tests was conducted in which small scale models of spinning turbine disk fragments were impacted against circular target rings. These tests were an extension of tests conducted at the Sandia National Laboratories and SRI International. The purpose of the overall program sponsored by the Electric Power Research Institute (EPRI) was to examine the impact phenomena associated with possible turbine disk failure.

In the Sandia program, 120° segments of full-scale turbine disks were impacted against target rings representative of the stator blade ring and outer turbine casing. Similar tests were conducted at SRI using one-fifth scale model disk fragments. In both of these programs, nonspinning, unbladed missiles were impacted against simple, symmetric target rings. The tests described in this paper were conducted to examine the effects of missile spin, blade crush, and target edge conditions on casing impact. One-eleventh scale model missiles were launched using a high speed spin chamber at the Naval Air Propulsion Center. The burst of a modified turbine rotor in the chamber provided simulation of both the rotational and translational velocities of steam turbine fragments. The turbine disks and blades had the same major dimensions and inertial properties as the prototype turbine disks and blades. The target was a 360° steel ring with dimensions scaled from those of the Sandia tests. In several tests, the target ring had a more complex, nonsymmetric cross section to simulate the support of the adjacent structure in an actual turbine casing.

In the first test, spinning, unbladed fragments were launched with the same initial (scaled) kinetic energies as that of the Sandia and SRI tests. The results showed that the residual energy of the spinning fragments was approximately the same as that of the nonspinning fragments launched in a piercing orientation. Tests with bladed fragments showed that for equal burst speeds, the residual energy of bladed fragments is less than that of unbladed fragments. The apparent effect of blades was to cushion the local impact and to increase the duration of the impact event, thereby reducing peak stresses and greatly increasing the strain energy absorbed by the target. Also, all or most of the blades were broken off at the root during perforation. In tests with nonsymmetric targets, it was apparent that the presence of the ring support structure resulted in greatly reduced deformation of the ring structure during impact. Secondly, bladed fragments impacting near the edge of the nonsymmetric target slipped off the edge prior to extensive ring deformation, resulting in much higher residual energy than for center impacts on symmetric targets.

1. Introduction

Though rare, failures of the shrunk-on disks in the low pressure sections of 1800 RPM steam turbines must be considered in the design of turbine casings and protective concrete structures in nuclear plants. The missiles produced by a ruptured turbine disk may be massive and possess high translational and rotational energies. Thus, it is important to understand the conditions under which disk fragments can escape from the turbine and the energy absorption capability of the casing structure.

Previous analytical and experimental attempts to quantify the energy absorption capability of turbine casings have examined the impact of a nonspinning, unbladed missile [1,2,3]. The spin energy has been accounted for by combining the rotational energy and the translational energy and converting the total into an enhanced translational energy with an elevated equivalent translational velocity. The blades have been neglected entirely. This approach greatly simplifies the analyses and the experimental techniques required, but does not completely model the physical impact event, leading to some question of the assumptions made in the previous work. Another previous experimental program [4] consisted of spin tests of unbladed missiles, but residual energy of the missiles after breakthrough was not measured.

2. Background

In prior experimental programs, tests have been conducted by Sandia National Laboratories [1,2] and SRI International [3]. For these tests, the Westinghouse turbine shown in Figure 1 was chosen as the prototype. The failure scenario assumed that the last stage disk would break into three equal segments and that each segment would move radially outward until it impacted the last stage stator blade ring and ring support. If the disk segment perforated the ring and ring support assembly, it would then impact the outer turbine casing. Simplified missile and target designs were chosen for the analytical and experimental studies of this scenario. A 120° segment of the prototype disk was chosen as the projectile but blades were not included. A steel semi-circular ring with rectangular cross section was chosen to represent the stator blade ring. The support from the adjacent casing structure was neglected. An outer cylindrical shell was chosen to represent the outer turbine casing.

Two full-scale casing tests were conducted at the rocket sled facility of Sandia National Laboratories [1,2]. The scenario for these tests assumed that the 1800 RPM turbines would fail at 120 percent of the design speed (1800 x 1.20 = 2160 RPM's), resulting in three equal disk segments moving radially outward, each spinning at the same rate as the disk prior to failure. Since there was no method available to produce the desired spin rate of the missile, spin energy was accounted for and converted to translational kinetic energy, thereby obtaining an enhanced translational impact velocity. One test was conducted with the missile oriented in the end-on or piercing orientation and the other with the missile in the side-on or blunt orientation. In the piercing test, the missile perforated both ring structures, retaining approximately one-third of its initial energy. The blunt impact case resulted in no perforation.

A similar set of casing impact tests was conducted by SRI [3] using 1/5-scale missile/target models. The missiles, which were 1/5-scale replica models of those in the Sandia tests, were launched by an explosively driven piston. The impact velocities and orientations closely replicated the full-scale tests. The results of these tests showed good agreement with the full-scale tests at Sandia and were instrumental in demonstrating the applicability of scaling in turbine missile impact testing.

3. NAPC Test Program

In the studies just discussed, prototype and replica disk segments were impacted against simplified, symmetric targets. Due to limitations of missile launch technique, rotation of the disk segments was not possible. Without proper spin, the response of the disk blades to impact could not be duplicated, so that blades were also absent in these tests. The resulting tests, though simplified from the actual case, gave an improved understanding of the impact event. The main objectives of the program [5] described in this paper were to examine the effects of missile spin and blade crush on casing impact. A secondary objective was to determine the effects of target support conditions on the response of the casing target to impact. One-eleventh scale model missiles were launched using the high-speed spin chambers at the Naval Air Propulsion Center in Trenton, New Jersey. The burst of a T-58 gas turbine rotor in the chamber provided scaled simulation of both the rotational and translational velocities of steam turbine fragments. The T-58 disks and blades were modified to have the same major dimensions and inertial properties as the prototype turbine disks and blades (Figure 2). The properties modeled included the outer hub thickness, outer radius, total mass, location of the centroid, and mass moment of inertia.

For most of the tests, the target was a 360° steel ring with dimensions 1/11 those of the inner ring used in the Sandia tests. For these symmetric target tests, the target ring was a replica model of the prototype Sandia inner ring; that is, all dimensions were scaled by the same factor, 10.9, and the same material was used. Figure 3 is a photograph of a bladed missile positioned inside this target. In the last three tests, the target ring had a more complex cross section to simulate the support of the adjacent structure in an actual turbine casing. This nonsymmetric target was designed to replicate more closely the stator ring support assembly, as seen in Figure 4. In this model, the symmetric target ring used previously was retained to represent the stator ring. The next stage stator ring and stator disk were replaced by an equivalent mass with the same centroidal location. The entire system was attached to a backup steel plate for support.

The ten tests conducted in this program were divided into two phases. In the first phase, seven tests were conducted with bladed and unbladed missiles impacting a simple, symmetric target ring. In these tests, the symmetric target rings were suspended freely by wires and were positioned to coincide with the model disk's plane of rotation. Three tests in the second phase were aimed at determining the effects of varying the impact location on the target and the effect of the target support structure on the impact event. For these tests, bladed disks were mounted in the nonsymmetric target and positioned to permit both edge impact and center impact on the ring section. Because of the desire to replicate the prototype ring boundary conditions in this test phase, the backup plate was attached directly to the spin chamber lid. Prior to mounting in the NAPC spin chamber, the disk was modified to fail at a preselected spin velocity in order to produce three equally shaped fragments at specified speeds up to 25,000 RPM's.

During the tests, a high-speed drum camera was used to obtain framing rates of 13,000 frames per second. The film records were used to determine missile rotational and translational velocities before target impact, orientation of the missile at time of impact, duration of the impact process, damage to the blades during impact, and the residual missile velocities. A summary of results from all successful tests is given in Table I. Values listed are averages for all three missiles launched in each test.

4. Results of Symmetric Target Tests

Three tests were conducted with unbladed missiles in this phase. EPRI-1 was conducted at a burst speed of 23,520 RPM's, which represents approximately 120 percent of the scaled prototype design speed (1800 RPM x 10.9 x 1.20 = 23,544 RPM). This burst speed corresponded to the scaled test conditions of the full-scale tests conducted at Sandia and the 1/5-scale tests conducted at SRI. All three missiles in this test perforated the symmetric target ring with significant translational and rotational velocities. Figure 5 presents a photograph of the EPRI-1 test taken after impact and perforation. The other two tests, EPRI-4 and EPRI-7, were conducted to establish the burst speed at which target perforation just occurs. It was determined that this burst speed was between 20,160 and 21,175 RPM's (1850 and 1940 RPM's for full-scale missiles).

For both tests in which perforation occurred, failure of the target occurred shortly after initial missile impact, prior to any significant deformation of the target ring. However, extensive ring deformation occurred after impact due to the kinetic energy imparted to the target during the impact event. This post-perforation deformation can be seen in Figure 5. Also of interest is a comparison of the energy dissipated by missiles during perforation. An examination of Table I reveals that more energy was dissipated during the perforation process by the higher energy missiles of EPRI-1.

Three tests were also conducted in this series using bladed missiles. EPRI-5 was conducted at 23,300 RPM's to allow direct comparison with EPRI-1. Since the missiles were contained in this test, EPRI-6 was launched at a burst speed of 25,200 RPM's. In this test, two of the three missiles perforated the target ring. Thus, the burst speed at which perforation just occurs for bladed missiles was seen to lie between 23,300 and 25,200 RPM's (2140 and 2310 RPM's). A late time photograph of EPRI-6 is given in Figure 6. In contrast to the results of the unbladed test, EPRI-1 (Figure 5), extensive deformation occurred prior to ring failure. Initiation of ring failure can be seen in the bottom right corner of Figure 6.

A review of Table I reveals that the bladed missiles possessed about three times more initial kinetic energy than the unbladed missiles. This was due to the greater mass, distance to the centroid, and moment of inertia of the bladed missile. The fact that the residual velocity for bladed missiles was less than that measured for unbladed missiles implies that there was much more energy dissipated during the impact of a bladed missile. Several factors probably combine to cause a much greater amount of missile kinetic energy to be dissipated in target perforation for the case of bladed missiles than for the case of unbladed missiles. From the film records, it was determined that extensive deformation of the target ring was caused by impact of the blades prior to actual contact with the outer rim of the missile hub. As a result, extensive distortion of the target occurred prior to target failure during perforation. This is in contrast to the impact of unbladed missiles for which target failure occurs almost instantaneously. This target distortion results in extensive dissipation of kinetic energy in elastic and plastic strain energy of the target. A second factor involved in energy dissipation is the deformation and fracture of the blades. During all three bladed tests, review of the high-speed films, such as seen in Figure 6, revealed that all or almost all blades were removed during the impact process. Post-test examination of the blades also revealed extensive blade deformation and multiple fractures in most blades. A third factor is that the presence of blades results in an increase of the distance from the center of the hub to the centroid of the missile. This increased centroidal distance results in an increased missile translational velocity, resulting in less missile rotation prior to impact of the disk rim on the target. The greater rotation of the unbladed missiles results in a more piercing orientation at impact.

5. Comparison of Symmetric Target Test Results

A comparison is made in Figure 7 between the spin tests conducted at approximately 120 percent design speed (23,540 RPM's) and the Sandia and SRI tests which were conducted in the piercing orientations. The piercing orientation for the nonspinning tests was chosen because it represented the upper bound of damage and because it most nearly corresponds to the actual orientation of a spinning missile upon impact. Since the current test program neglected the outer turbine casing, the Sandia and SRI data considered in Figure 7 correspond to perforation of the ring prior to impact of the outer shell. The actual values measured in the Sandia test are given in the figure. The results from the 1/5-scale SRI tests and the 1/11-scale tests of this program have been scaled to correspond to full-scale values.

The results are quite interesting. The fact that the results from the 1/5-scale SRI test matched those of the full-scale Sandia test adds confidence to the use of small-scale models. With this in mind, the effect of projectile spin can be seen directly by comparing the results of the nonspinning Sandia and SRI tests and EPRI-1. For equal initial kinetic energies, all three tests had comparable total residual energies. However, 30 percent of the residual energy of the spinning missile was in the form of rotational energy. The effects of blades on the impact process can be seen directly by comparing the results of EPRI-1 and EPRI-5. Though having comparable burst speeds, the initial kinetic energy of the bladed disk was almost three times greater than that of the unbladed disk. However, the bladed missiles were unable to perforate the target ring. The energy dissipation mechanisms associated with blade impact more than compensate for the increased initial kinetic energies. A very different result is seen for the impact of bladed missiles onto the edge of the nonsymmetric targets. The total residual energy of each missile was greater than for any of the other four tests displayed in Figure 7. The residual translational energy was also found to be within 10 percent of that measured for the nonspinning tests.

6. Results of Nonsymmetric Target Tests

Two successful tests were completed in this phase of the program. EPRI-8 involved the impact of bladed missiles on the edge of the target ring, while EPRI-10 involved bladed missiles impacting the center of the ring. Both tests were conducted at burst speeds of approximately 23,780 RPM's, thereby allowing direct comparison with EPRI-1 and EPRI-5. It was apparent in the high-speed films that edge impact of the missiles allowed them to slide off the deflecting edge of the target ring. This resulted in less missile kinetic energy being dissipated in target deformation and fracture as well as the loss of fewer blades. The edge impact with the accompanying target deflection also resulted in a 15° deviation of the missiles from the original trajectory plane. In the center impact test, EPRI-10, one missile was apparently contained and the other two perforated the ring. Failure of the high-speed camera resulted in no residual velocity information. However, post-test examinations led to the following conclusions: (1) one missile broke through the ring with significant residual energy but was deflected approximately 9° from the plane of its original trajectory, (2) one missile broke through the ring with less residual energy and was deflected almost 66°, and (3) the third missile failed to perforate the target ring.

7. Conclusions

The following conclusions can be made from this program:

- The mitigating effects of blades in absorbing energy and cushioning impact more than compensate for the increase in mass and moment of inertia.
- Therefore, in predicting exit conditions, neglect of the blades during impact appears conservative.
- For unbladed fragments, it appears valid to assume that a good estimate of the total energy absorbed in ring perforation can be obtained using a nonspinning fragment with a resultant translational energy equal to the sum of the initial translational and rotational energies of a spinning fragment.
- It appears reasonable to neglect the mass of the blades in predicting the residual mass of the fragment which has exited the casing.
- The effect of impacting the target near the edge is to increase the residual energy of the fragments.

8. References

[1] Yoshimura, H. R. and Schamaun, J. T., "Full-Scale Turbine Missile Casing Tests," EPRI Final Report NP-2741, (January 1983).

[2] Yoshimura, H. R., Schamaun, J. T., and Sliter, G. E., "Full-Scale Turbine-Missile Casing Exit Tests," Proceedings of the Fifth International Conference on Structural Mechanics in Reactor Technology, Berlin, Germany, August 13-17, 1979, Paper No. J8/12.

[3] Romander, C. M. and Florence, A. L., "Scale-Model Turbine-Missile Casing Impact Tests," EPRI Final Report NP-2742, (January 1983).

[4] Hagg, A. C. and Sankey, G. O., "Containment of Disk Burst Fragments by Cylindrical Shells," Journal of Engineering Power, Trans. ASME, Series A, Volume 96, (2), pp. 114-123, (1974).

[5] Wilbeck, J. S., "Spinning Turbine Fragment Impacts on Casing Models," EPRI Final Report NP-2743, (March 1983).

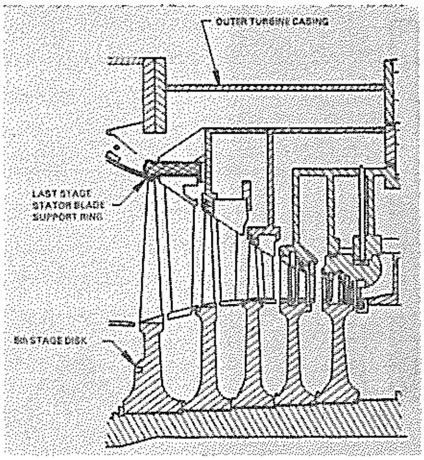

Figure 1. Prototype Turbine

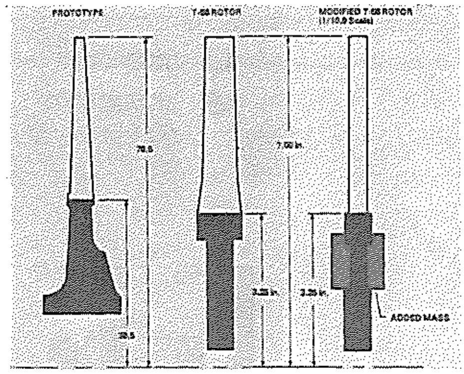

Figure 2. Modified T-58 Rotor Design

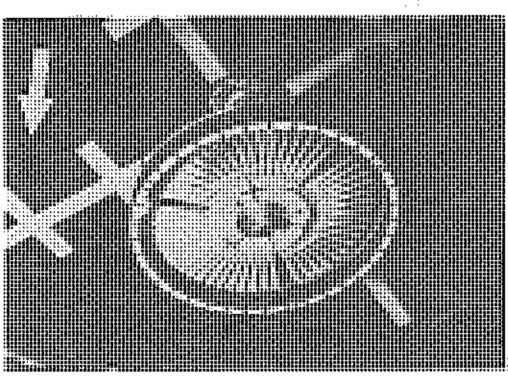

Figure 3. Bladed Disk Positioned in a Symmetric Target Ring

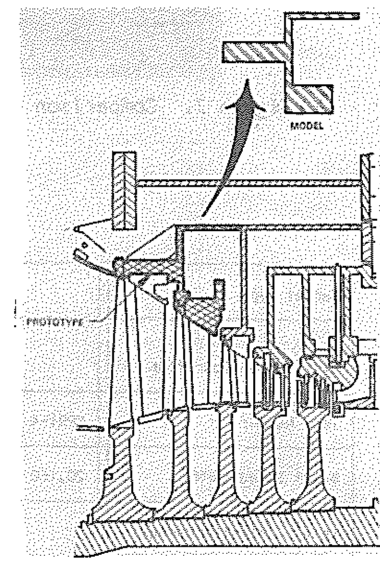

Figure 4. Prototype/Model of the Nonsymmetric Target

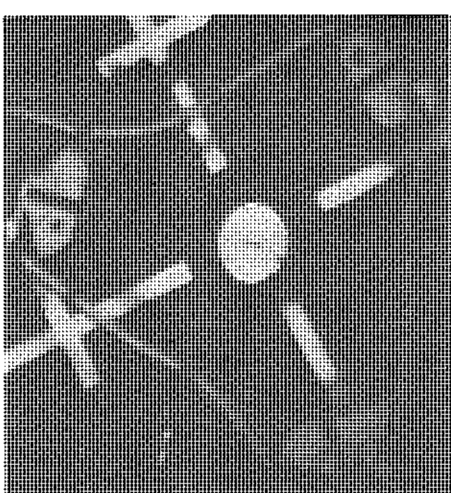

Figure 5. EPRI-1, Unbladed Missile Impacting a Symmetric Target at 120 Percent of Design Speed

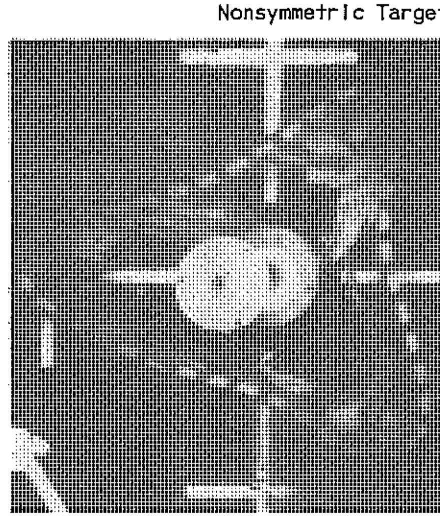

Figure 6. EPRI-6, Bladed Missile Impacting a Symmetric Target at 128 Percent of Design Speed

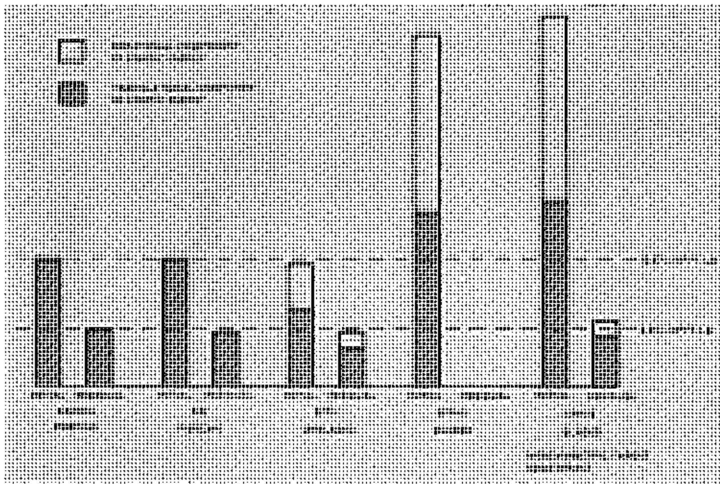

Figure 7. Comparison of Spin Tests With Sandia and SRI Piercing Tests

Table I. Summary of Results

Target Type	Symmetric Ring						Nonsymmetric Ring	
Missile Configuration	Unbladed			Bladed			Bladed	Bladed: Edge Impact
Test Number	EPRI-4	EPRI-7	EPRI-1	EPRI-2	EPRI-5	EPRI-6	EPRI-10	EPRI-8
Burst Speed (RPM)	20,160	21,175	23,520	18,810	23,300	25,200	23,765	23,780
Initial Missile Energy:								
Translational (ft-lb)	4,096	4,796	5,971	9,935	13,275	16,718	13,810	14,095
Rotational (ft-lb)	2,411	2,659	3,282	8,670	13,302	15,560	13,838	13,856
Total (ft-lb)	6,507	7,455	9,253	18,605	26,577	32,278	27,648	27,951
Residual Missile Energy:								
Translational (ft-lb)	0	1,396	3,019	0	0	1,313	Unknown	3,921
Rotational (ft-lb)	0	664	1,236	0	0	150	Unknown	1,070
Total (ft-lb)	0	2,060	4,255	0	0	1,463	Unknown	4,991